

3.4 EXPERIMENTAL PROCEDURE

Six specimens were tested in this investigation. In each case, the preparation required the following steps:

1. Cutting the initial notch in the bottom plate.
2. Bolting the specimen to the support structure.
3. Installing the splice plates to provide for a more continuous structure.
4. Mounting strain gages in the bottom plate of the specimen.

The testing of each specimen ranged from 3-6 weeks at a cycling frequency of 1.2 Hz. Each specimen endured between 1.5 million and 3.5 million cycles before failure was concluded. At no point was unstable crack propagation observed. Rather, incremental crack growth was similar in many of the cases.

To record the crack growth during testing, a red penetrating dye was used. The dye is sprayed around the region of the crack tip and allowed to permeate any imperfections in the material. After several minutes, the dye is removed from the surface with a degreasing agent and a dry cloth. Soon after the surface is cleaned, the dye may re-emerge from the cracked areas either through dispersion or with the aid of a developer. The developer is an agent that is sprayed on the cleaned surface that turns white when dried. It is stained by any red dye that emerges from the crack. Figure 3-16 shows the use of the procedure to identify the crack tip in the baseline specimen.

The use of the red dye to locate the crack tips is particularly effective during testing. Once the surface has been wiped clean, the permeated dye is forced out during cycling. This phenomenon, commonly referred to as pumping, provides an easy means for finding the crack tip.

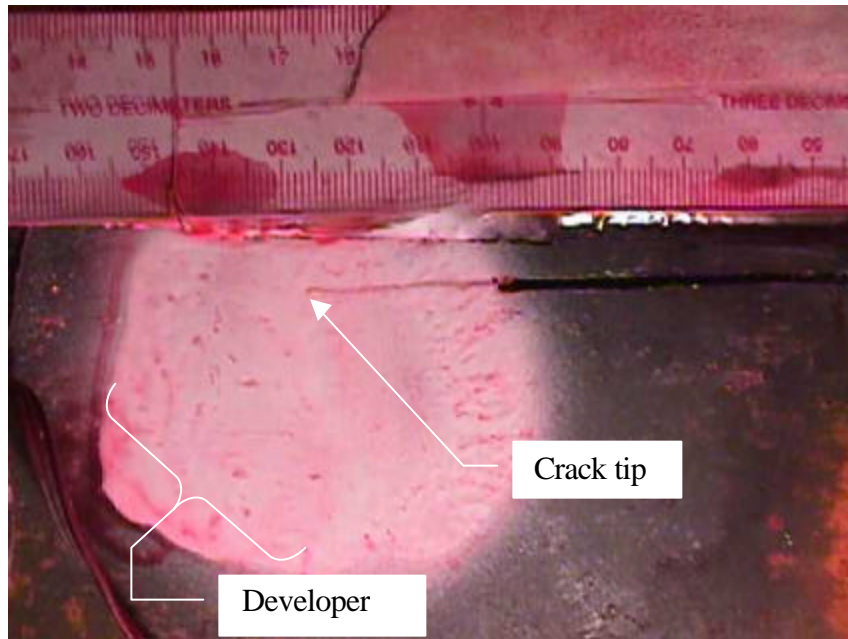


Figure 3-16: Use of red dye penetrant and developer to locate crack tip.



Figure 3-17: Crack growing in stiffener of case 3.

In the stiffened panel cases, excluding case 2a, an oval viewport was flame cut in the top flange of the specimens (See Figure 3-13). This viewport increased the applied stresses in

the specimen slightly while allowing one to record the crack growth in the stiffeners from the interior of the box section plate (See Figure 3-17). It was found that the distance of the two crack tips, the one in the stiffener and the one in the plate, from the stiffener to plate intersection was usually about the same. In every case, the growth in the stiffeners virtually matched that of the plate until the stiffener cracks reached approximately $\frac{3}{4}$ of the height of the stiffener webs.

The stiffeners were never completely severed in the test cases. This shortcoming was due to both shear lag effects across the bottom plate and the restraint of the edge webs. To quantify the magnitude of the shear lag effect, stress readings were taken at the top of the stiffener webs before significant cracking occurred. These initial stress readings indicated that the interior stiffeners experienced stress ranges significantly lower than that of the plate. In fact, while the plate was cycled at a stress range of 45 MPa the interior stiffeners only experienced 4 MPa. The exterior stiffeners exhibited greater uniformity with the plate with initial stress ranges of 35 MPa.

The restraint of the edge webs also contributed largely to the lack of stiffener separation. The crack could not be opened wide enough for crack growth to continue in the stiffeners because the edge webs limited the crack opening displacements. This drawback could have been avoided only with a wider and deeper specimen. The loading limitations of the equipment, however, would make such a configuration impossible without scaling down the relative thickness of the shapes used in both the support structure and the specimens.

The lack of stiffener separation does not constitute a failure of the experiments. Actually, the behavior allowed the prediction of a realistic case in which shear lag effects in a structurally redundant system are to be considered. The portion of the stiffener that was severed contributed to crack propagation. The uncracked portion of the flanges, on the other hand, provided little restraint and the cyclic opening of the crack merely pivoted about the horizontal flange like a hinge. An end result to the lower stresses in the stiffeners was to

lower the effective stiffener area as it affects crack growth. This point will be discussed in Section 8.3 (Page 153).

Throughout the testing the effects of load shedding were studied by monitoring local stress levels and overall deflection. The prominence of load shedding is characteristic of a structurally redundant system. Load shedding was observed to a great extent in the experiments as the crack progressed through the bottom plate. Normally one would observe increased deflections proportional to the reduction in the net section as the crack propagates. The multiple load paths present in the composite section limited the displacements observed. A maximum mid-span deflection prior to bottom plate cracking was approximately 20-mm. Only a 6-mm increase in deflection was noted after the crack had propagated into a through-thickness crack in the edge web (See Figure 3-18). This small increase could be attributed to the bolt up design of the experiments; however, no slip was detected between the specimen/support beam interface.

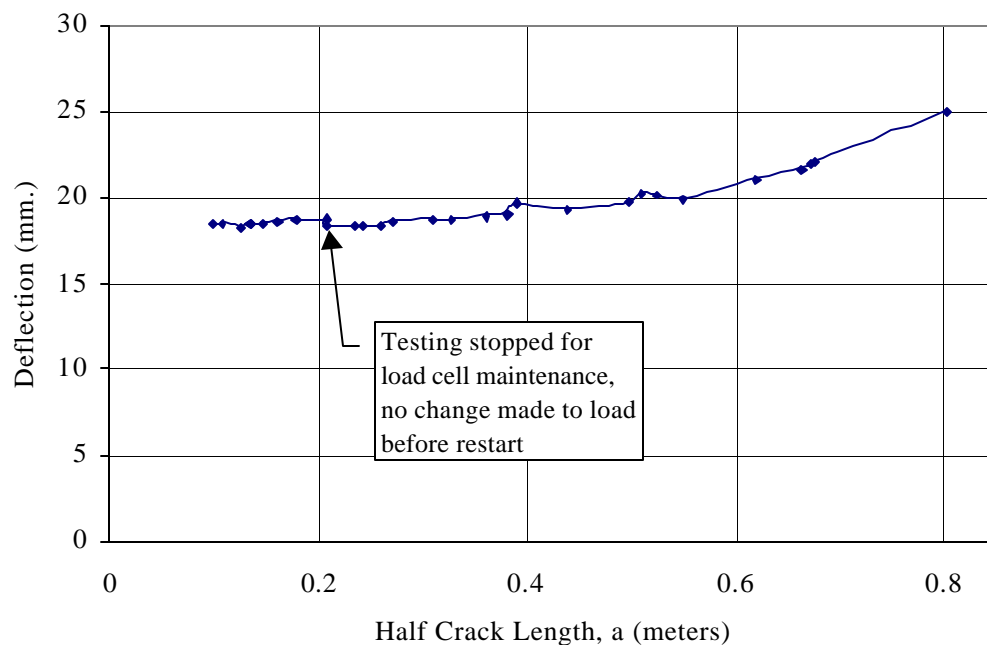


Figure 3-18: Maximum deflections incurred during testing.

3.5 RESIDUAL STRESS MEASUREMENTS

Residual stresses were theorized to affect fatigue crack propagation rates significantly. To quantify the residual stress present in the experiments, residual stress measurements were made on two of the specimens using the sectioning method. Each specimen was sectioned using 41 coupons with a nominal gage length of 254-mm. Four coupons from either side of each stiffener were taken with a width of 12-mm. In addition, three coupons with a width of 37-mm were taken from the region between stiffeners. The residual stress measurements were made using previously tested panels two and three.

The well-established procedure of sectioning was chosen to be the most economical and convenient method for measuring residual stress. Prior to extraction, gage points were marked at mid-distance between a free edge of the stiffened panel and the crack line. The gage points were then drilled approximately 7-mm deep with a #2 center drill bit (~3-mm diameter). Using a digital Whitmore gage with accuracy to 0.1-mm, the distance between the gage points was obtained and an average of three readings was used. After the initial readings were taken, the full section containing the gage points was removed from the specimen. Each coupon was extracted from the larger section with a bandsaw that was cooled with a steady flow of cutting fluid. After the coupons were removed, final readings were obtained by once again averaging three readings. Figure 3-19 shows the extracted coupons taken from one of the specimens.

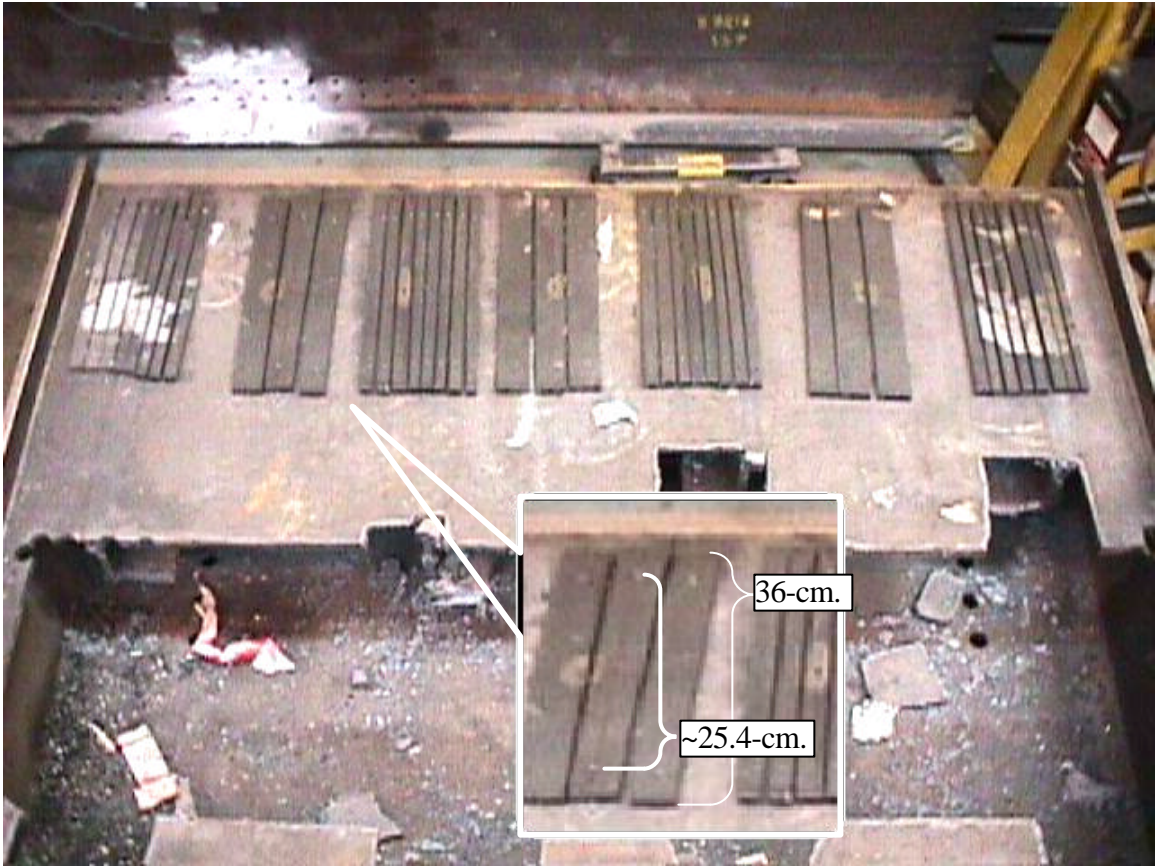


Figure 3-19: Sectioning coupons used for measuring residual stress distributions.

The measured residual stress fields are shown in Figure 3-20. Equilibrium requires offsetting areas of tensile and compressive stress to balance in the specimen. As one may notice, the measured residual stress distribution does not satisfy equilibrium. This discrepancy is likely due to the accuracy of the measurements as well as a minute amount of residual stress-induced curvature in the coupons. A more probable plot of residual stress could be obtained by lowering the x-axis by 60 MPa.

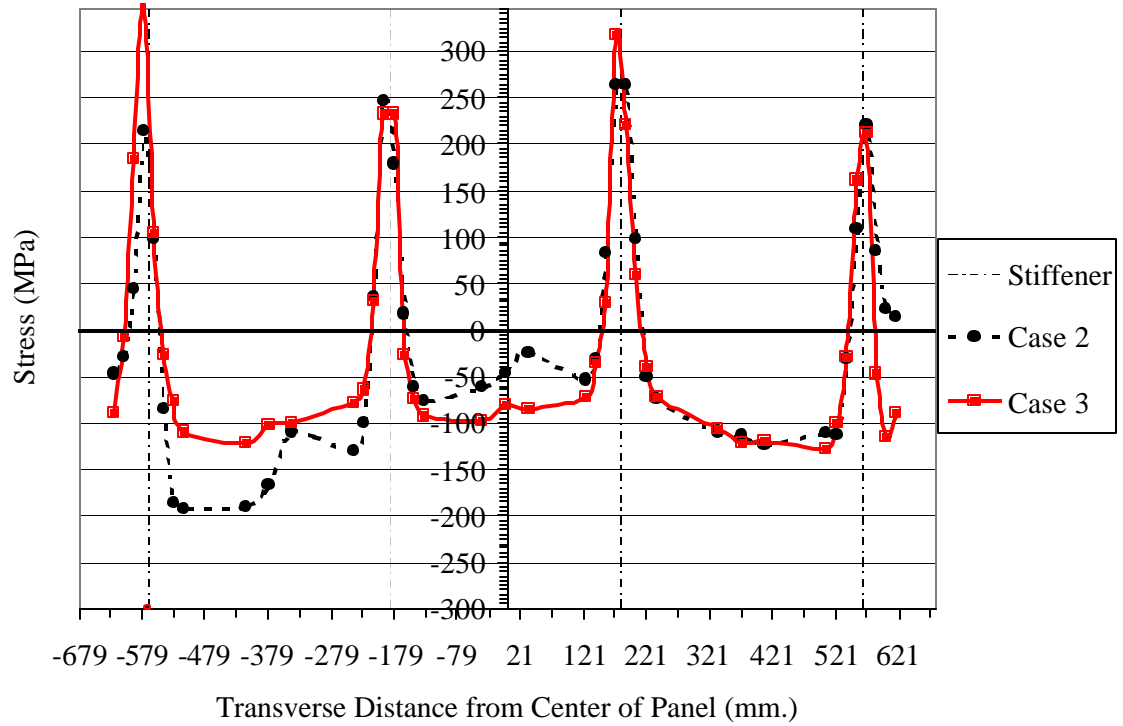


Figure 3-20: Residual stress distributions measured in two specimens.

Faulkner's model for residual stress distribution will be utilized as a simple representation of the actual residual stress in the specimens (See Figure 3-21). This model, as discussed in chapter 3, models the tensile regions around the stiffeners as triangular shapes with a base width proportional to the plate thickness (η). The triangular width typical of as-built ship structures ranges from 3.5 to 4 times the plate width, while values between 3 and 3.5 are more typical of ships after shakedown. The analytical program developed includes a routine for developing the Faulkner representation based on the yield strength of the material, the plate thickness and η .

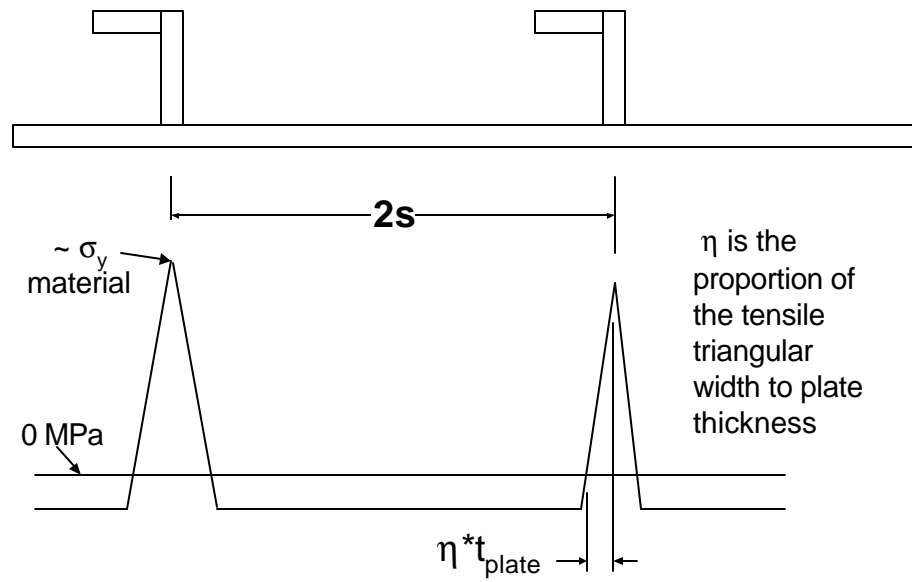


Figure 3-21: Faulkner model for residual stresses.

4 Experimental Results

4.1 BASELINE CASE

The first specimen tested was the baseline specimen, which consisted of a hollow specimen without stiffeners on the bottom plate. Initially a 204-mm notch was cut in the center of the specimen. After 300,000 cycles measurable crack growth could not be detected. In order to facilitate a crack formation the notch was beveled through the thickness at a thirty-degree angle. The beveling technique successfully initiated crack tips at the notch ends and the crack then grew 2-mm in 20,000 cycles.

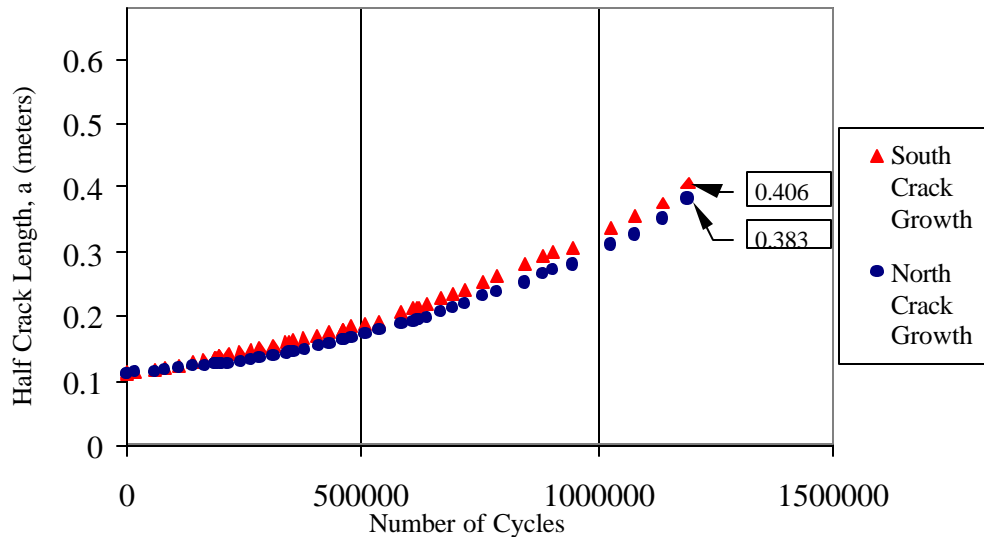


Figure 4-1: Baseline test case data.

The strain gage readings indicated an average applied stress range of 29 MPa. Slow crack growth was noted at this applied stress range and crack size, and at 540,000 cycles the loading range was increased to achieve an average applied stress range of 33 MPa. These stress range values were obtained by taking the average of the center and outer strain gage measurements, whose location was 76-cm from the crack line (See Figure 3-7).

The baseline test was stopped short of the full panel width in order to adhere to a rigorous testing schedule. Its termination was tolerated because the behavior observed was close to what was expected for a CCT specimen. Figure 4-1 shows the complete results of the test.

4.2 OVERVIEW OF STIFFENED PANELS TEST RESULTS

Each stiffened panel was tested under the same loading conditions and frequency. The starting crack length for each specimen was varied because of difficulties initiating a crack within a reasonable number of cycles ($\leq \sim 500,000$ cycles). The performance of all the cases, except case2a, can be seen in Figure 4-2. The plot has been constructed to align the crack growth stages, and thus the number of cycles for each test case is shifted horizontally to align its initial crack length with that of case four.

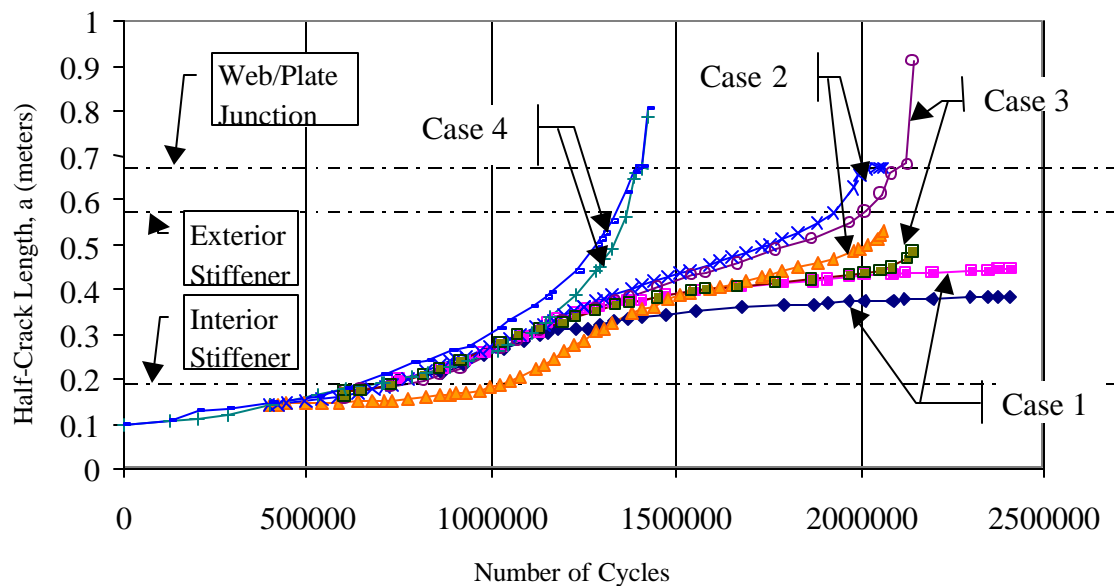


Figure 4-2: Stiffened panel test data (Excluding case 2a).

One will notice a distinct similarity between cases two and three. These tests involved stiffeners with ratholes (Case 2) and raised drain holes (Case 3) along the crack path. Case 4

exhibited no retardation effects due to the stiffeners or internal residual stress. Case 1 (Solid stiffeners) did show significant retardation effects, although the last five data points represent a gradual loss in applied stress due to cracking elsewhere in the specimen. The details of each test will be further discussed in the following sections.

4.3 CASE 1: SOLID STIFFENERS

A stiffened panel with solid stiffeners was investigated in test case one. This case represents a situation where an existing crack propagates into a solid stiffener. An initial notch of 28-cm, with a through-thickness bevel, was cut into the specimen and 418,000 cycles accrued with no noticeable crack initiation. At this point, the initial notch was lengthened to 30-cm and testing resumed. Cracking had still not initiated at 1,032,500 cycles. Once again the beveled notch ends were manually advanced, this time to a total notch length of 33-cm, but no crack tip formations were noticed even after an additional 400,000 cycles. Finally, the crack was manually extending to a total sawcut length of 40-cm, a distance which took the initial notch partially into the solid stiffener. With this crack length, crack tips readily formed within 100,000 cycles and the testing was considered officially under way.

The difficulty initiating the crack in this case is a testament to high compressive residual stress and the beneficial restraint of the stiffeners. Modeling observations indicate it is likely that the compressive residual stress played a larger role in crack retardation than the restraint of the stiffener. These observations will be discussed in Section 8.3 (Page 151).

The testing results can be seen in Figure 4-3. Initial crack lengths were identical in both the north and south directions, and variations in growth are the result of variations in residual stress and minute unsymmetrical loading.

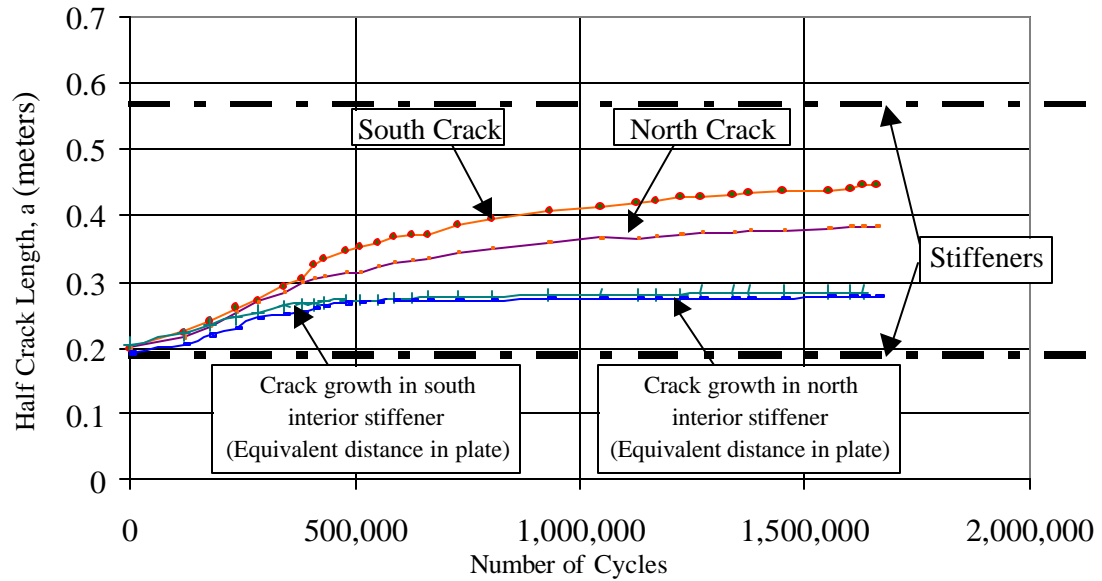
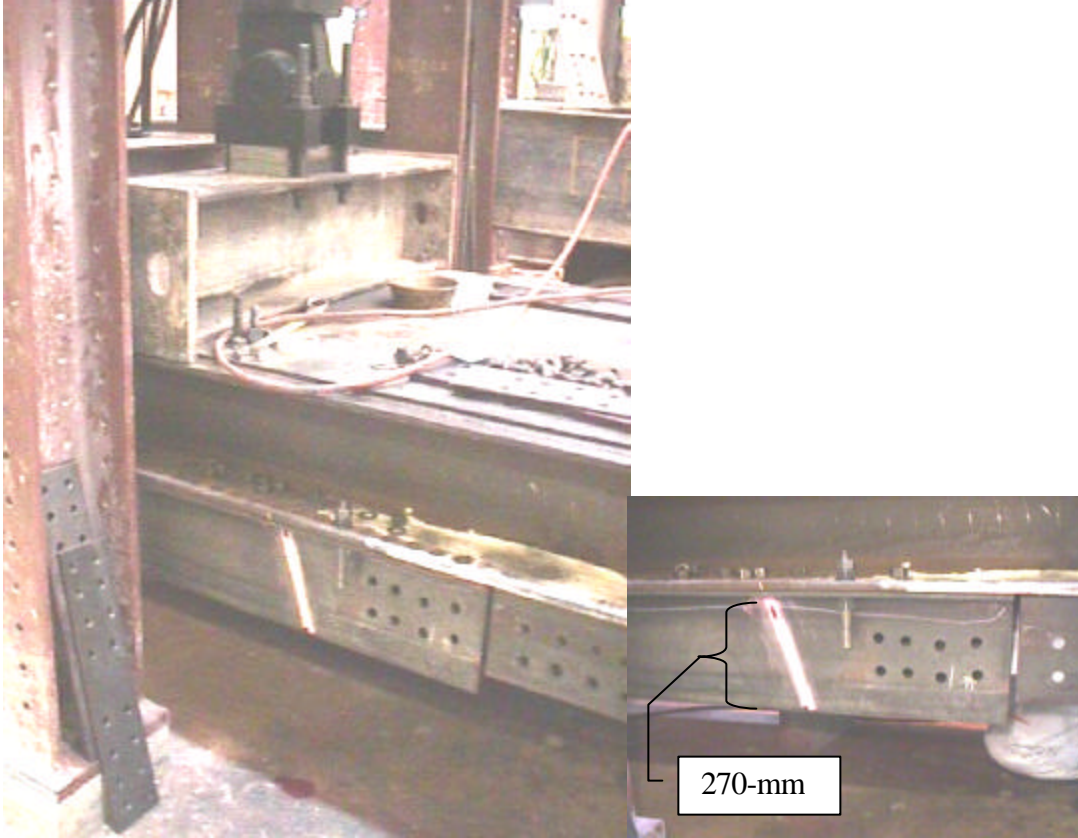


Figure 4-3: Case 1 experiment data.

During the latter part of the test, rubbing along the west end splice plates caused cracking in the edge webs away from the centerline of the specimen (See Figures 4-4,5). The cause of the rubbing was the use of 6-mm thick spacer plates used between the specimen and the splice plates at these locations. The spacer plates became necessary because of small variances in the alignment of the specimen webs. Cracking at these locations reduced the effectiveness of the force transfer into the specimen, and the last four data points reflect diminished stress levels as the remote cracking ensued.



Figures 4-4, 5: Edge web cracking due to rubbing in case one.

As reported earlier, the crack growth in the stiffeners matched that of the plate up to approximately three-fourths of the stiffener height. Cracking in the plate stalled prior to reaching the exterior stiffeners. Stress levels in the plate were monitored and found to be constant up until the last four data points. For this reason, the decrease in growth rate is attributed to the effects of high compressive residual stress; similar to the initial difficulties encountered trying to initiate a crack. Regrettably, no residual stress measurements were obtained from this specimen to quantify the internal compressive stress.

4.4 CASE 2 AND CASE 3: STIFFENERS WITH CUTOUTS AND CENTRAL NOTCHES

Cases 2 and 3 represent a variety of cutouts found commonly in ship structure. Case 2 simulates regions where ratholes are incorporated. Case 3 contains a raised drain hole. These two tests performed very similarly, with mild crack retardation effects from the stiffeners.

Case two test results may be seen in Figure 4-6. This test started with a manually cut crack length of 20 cm. Only eight millimeters of growth was observed in 980,000 cycles. The rate of growth was documented and then the crack was manually advanced to 28-cm. total length to promote a tolerable test duration. Figure 4-6 shows the crack behavior from this point forward. Crack growth sped up considerably with this new notch length.

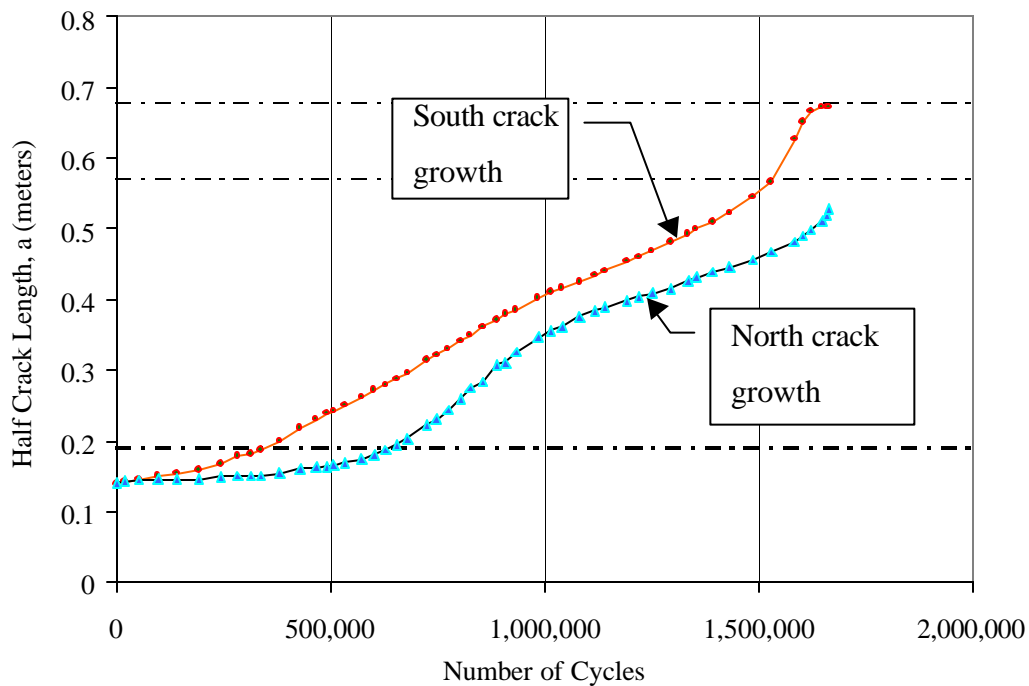


Figure 4-6: Case 2 experiment data.

No measurements were taken of the crack growth in the stiffeners for this test case. The test was completed when the crack had propagated to within 50-mm of the specimen's top plate. Final crack lengths may be seen in Figure 4-7.

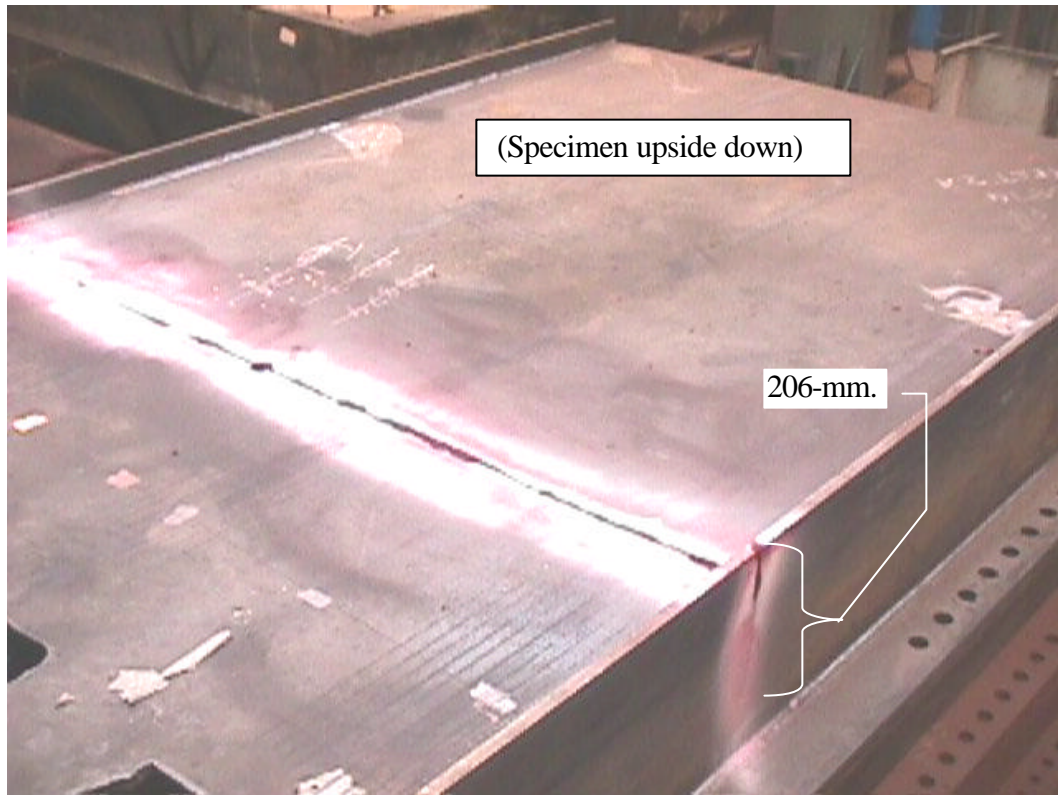


Figure 4-7: Case 2 at failure.

Case 3 exhibited remarkably similar test results. The initial notch length was 155-mm in either direction of the centerline. Once again, this initial crack length proved insufficient to propagate a solidly propagating crack. At 100,000 cycles, the crack was lengthened with a reciprocating saw to a total length of 35-cm. This notch length facilitated more rapid growth and 8-mm of growth was seen in either direction of the plate within 100,000 cycles. This growth marked the true start of the monitored propagation. A full profile of the test results may be seen in Figure 4-8.

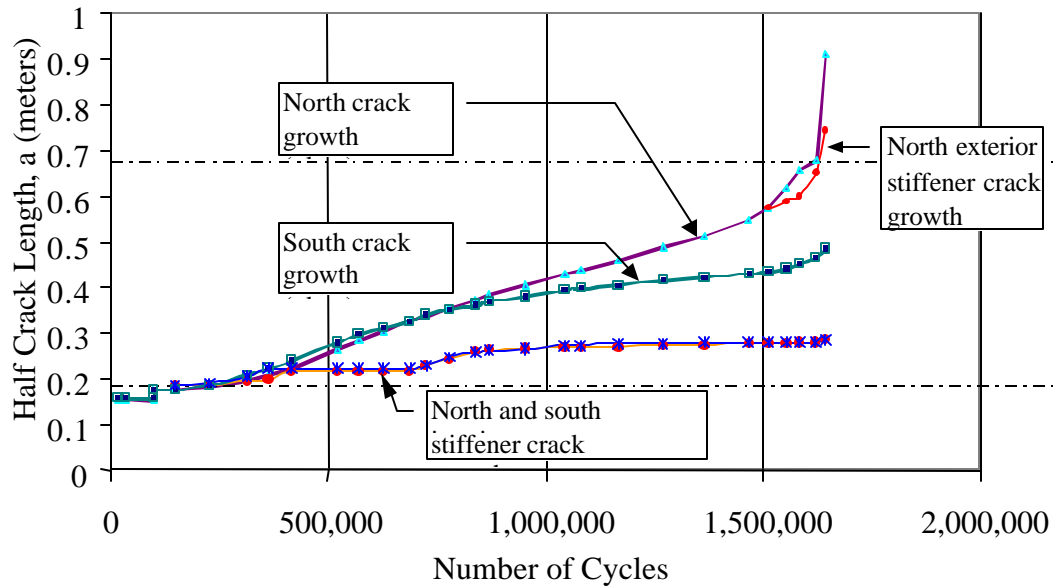


Figure 4-8: Case 3 experiment data.

One may notice the south crack data decreases its growth rate around 750,000 cycles. This deviation from the northern crack growth is a direct result of splice plate cracking in the southeast corner of the experimental setup. The interior splice plate at this location suffered a fatigue crack of its own and led to slightly decreased stress values on the south side of the specimen. The change in stress due the splice plate cracking averaged 6 MPa lower than that of the intact splice plate. For this reason, the south crack growth was significantly retarded compared to that of the north crack.

Earlier the similarities between case 2 and case 3 were noted. Figure 4-9 shows both tests on the same plot.

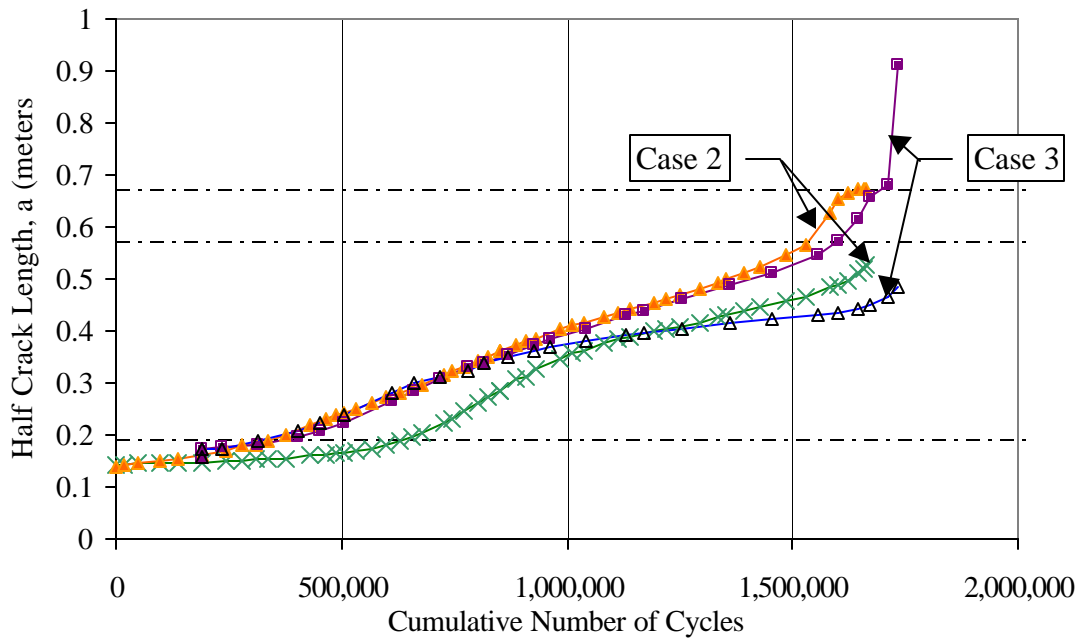


Figure 4-9: Performance similarities of cases two and three.

Only small differences exist between the cases. Previously it was observed that the crack propagation rate for the south tip in case three diminished due to remote cracking in the splice plates and a corresponding stress drop. In case two, however, the opposite behavior is noted with the southern crack tip outpacing the northern tip with no stress fluctuations observed. This behavior signifies that an appropriate growth scenario may be extrapolated from the worst case scenarios.

4.5 CASE 4: PLATE WITH BUTT WELD AND STIFFENERS WITH RATHOLES

Case four represents a master butt joint in ship structure where two sections of prefabricated hull are joined. It was originally anticipated that the difficulty starting a crack would again be repeated with this specimen. Surprisingly, the 20-cm initial notch was immediately successful in starting crack growth. Within 100,000 cycles an 8-mm crack had formed and was propagating well.

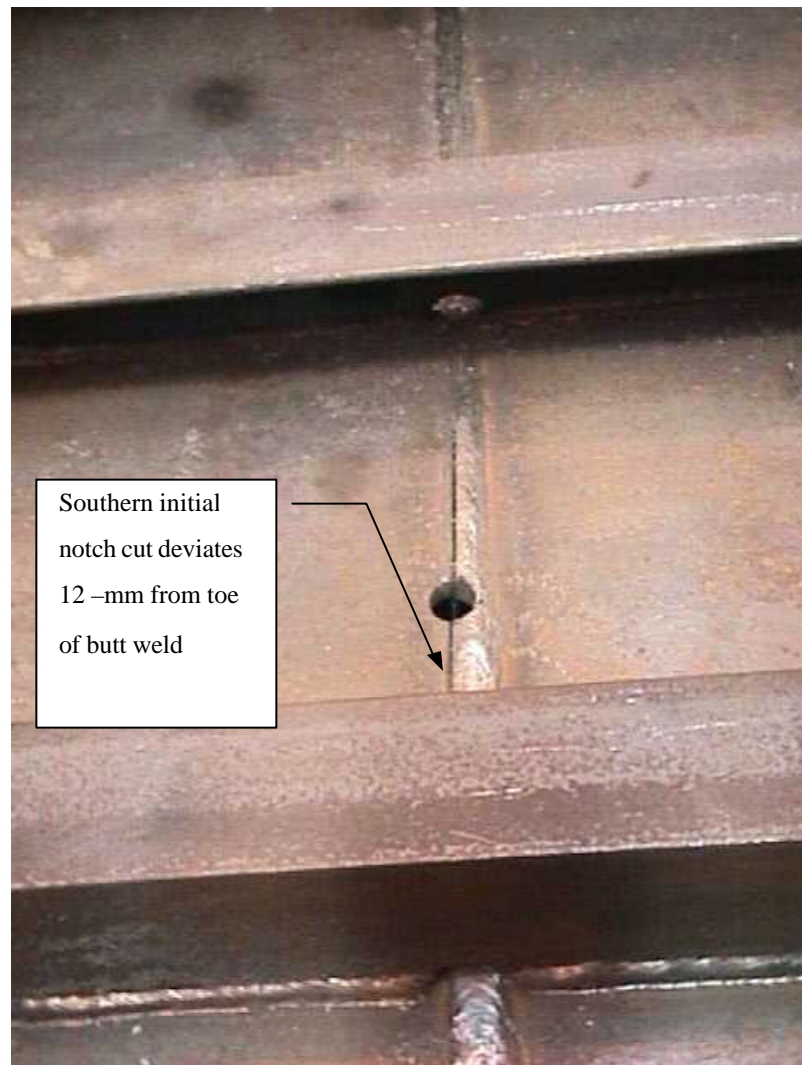


Figure 4-10: South notch end deviates from butt weld.

Rapid initiation was observed even on the southern side of the specimen where the saw-cut notch had inadvertently deviated from the butt weld by almost 12-mm. The crack that initiated away from the toe of the butt weld continued to run parallel to the butt weld for the majority of the experiment.

Crack growth was significantly higher than that of the other specimens including the baseline case. Such ease of crack initiation demonstrates the fatigue sensitivity of this type of detail in ship structure. While unstable crack growth was never observed, the beneficial

effects of any internal compressive stress due to the stiffener fillet welds were negated by the butt weld. Furthermore, the stiffeners themselves provided no retardation effects on the crack growth. In this test, the internal stiffeners still exhibited lower stresses from shear lag in the specimen, as previously discussed in Section 3.4. If the stiffeners had experienced stress levels similar to that of the plate, crack growth would be amplified by the gradual loss of stiffener load-carrying capacity. The complete test results may be seen in Figure 4-11.

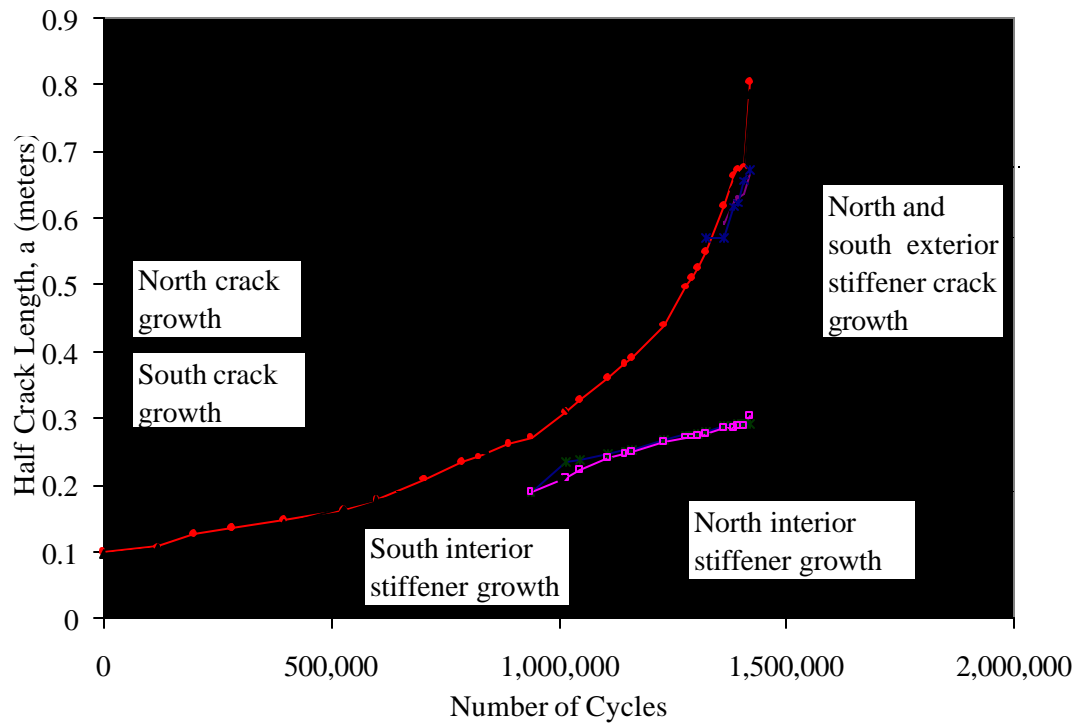


Figure 4-11: Experimental results for case four.

4.6 CASE 2A: MULTIPLE SITE DAMAGE IN STIFFENED PANELS WITH RATHOLES

In many instances in ship structure, cracks initiate at fillet weld terminations near ratholes used for weld access or drainage. Furthermore, cracks at these locations are often prevalent in adjacent stiffeners experiencing the same loading conditions. Case 2a attempts to

simulate the propagation behavior that might occur in this situation. This initial cracking scenario is the most realistic among the specimen configurations.

There were many concerns about the proper treatment of this situation given the experimentation setup. First of all, the stress gradient across the bottom of the panel required unequal crack lengths in order to duplicate four simultaneous running cracks. Because the stress levels near the edges of the panel were 50 percent higher than those in the middle of the panel, it was decided to make the initial interior crack lengths significantly longer than those under the exterior stiffeners. The reasoning for this was the concern that the exterior cracks would propagate through the edge web before the interior cracks showed any significant growth. Another concern was the feasibility of all four cracks behaving realistically in an environment where unequal notches were artificially introduced. The testing configuration could not reasonably be changed, and thus the test was carried out with unequal notches whose lengths were set to minimize the effects of shear lag. The initial notch lengths can be seen in Figure 4-12.

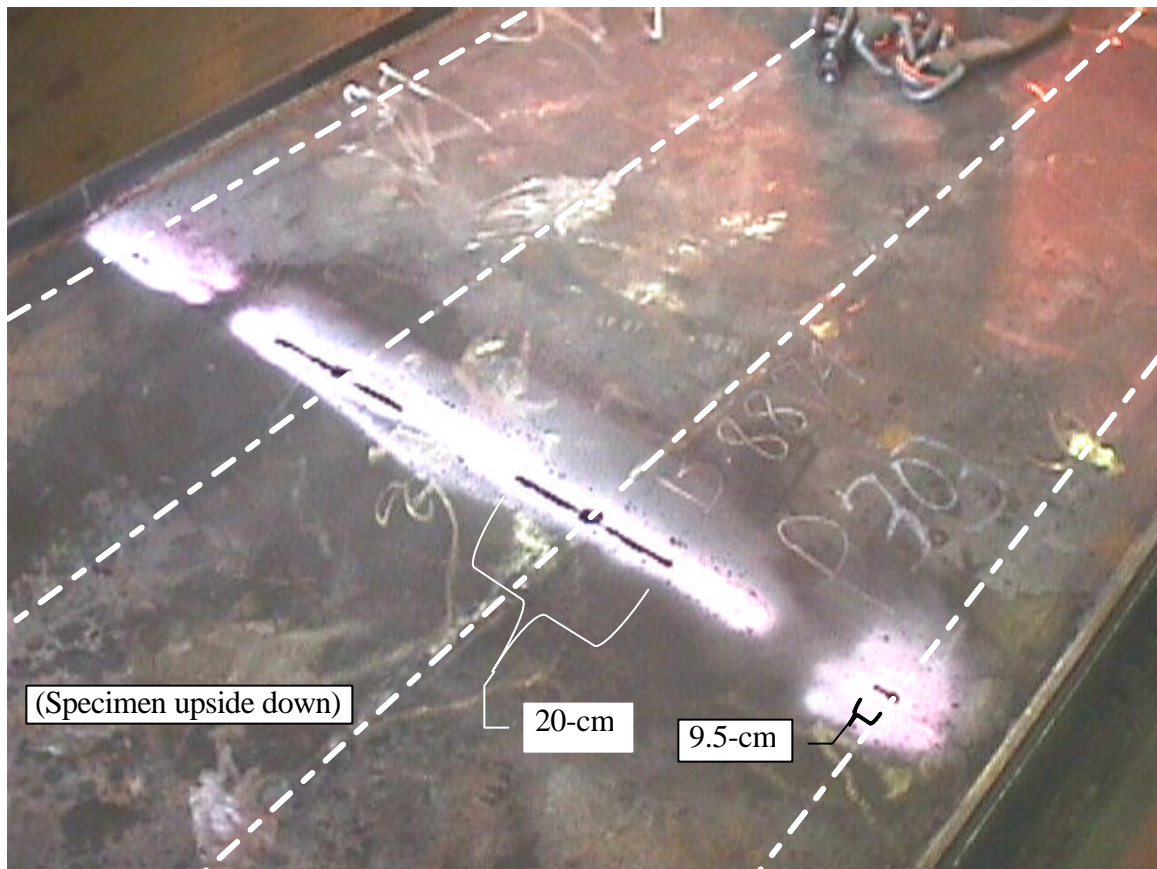


Figure 4-12: Initial crack lengths used in specimen 2a.

The test data for the plate crack growth may be seen in Figure 4-13. The figure displays the whole panel width and the crack length progression. As one can see, the exterior crack lengths proved to be too small to grow a crack with ease, while the interior crack tips grew at a relatively slow rate. In fact, the interior cracks grew consistently while the exterior cracks had to be manually extended in increments before self-propagation occurred. The length at which the exterior cracks became self-propagating was 10-cm. At this point, the interior cracks had grown to a total length of 27.4-cm. The remainder of the test displayed very symmetric results that yielded identical growth rates in the exterior and interior cracks.

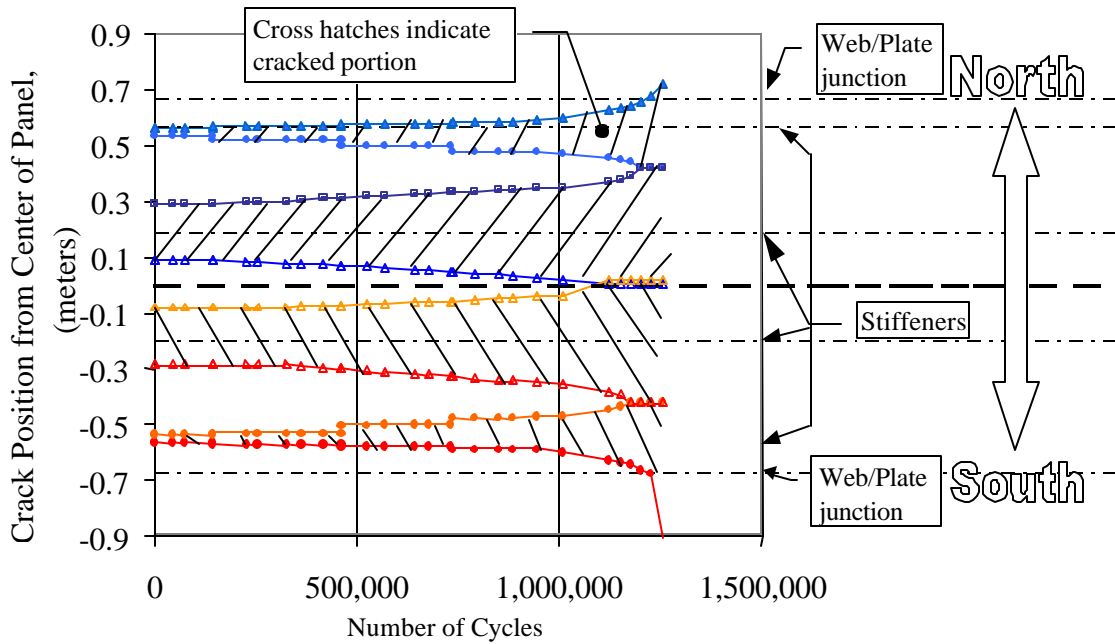


Figure 4-13: Initial crack lengths used in specimen 2a.

The exterior crack growth rates remained fairly slow until all the interior crack tips joined. This behavior could be expected as the intact plate sections minimize crack opening displacements until the cracks merge.